Ultraviolet–Visible Spectroscopic Studies on Manganese and Rhenium Oxide Fluorides in Low-temperature Matrices

Alan K. Brisdon,[a] John H. Holloway,[a] Eric G. Hope,*[,a] Paul J. Townson,[a] William Levason[b] and J. Steven Ogden[b]
[a] *Department of Chemistry, The University, Leicester LE1 7RH, UK*
[b] *Department of Chemistry, The University, Southampton SO9 5NH, UK*

Five high-oxidation-state metal oxide fluorides, MnO_3F, ReO_3F, ReO_2F_3, $ReOF_5$ and $ReOF_4$ have been isolated as molecular species in inert-gas matrices at low temperatures, and studied by IR and UV/VIS spectroscopy. In particular, the electronic spectra are described and the principal charge-transfer bands assigned using the optical electronegativity model. This suggested that a new value for $\chi_{opt}(F^-)$ of 3.6 is appropriate for transition-metal oxide fluorides.

There are four oxide fluorides of rhenium, ReO_3F, ReO_2F_3, $ReOF_5$ and $ReOF_4$, and one of manganese, MnO_3F, all of which are noted for their reactivity. Previous spectroscopic studies[1–5] indicate that all can exist as monomers in the vapour phase. The present work is a continuation of our studies on the complete characterisation of high-oxidation-state fluorides[6–9] and oxide fluorides[10–13] using the combination of matrix-isolation and IR and UV/VIS spectroscopic techniques. The advantages offered lie first in the low-temperature stabilisation of the highly reactive monomers that the matrix-isolation technique affords, and secondly in the relatively narrow linewidths and cumulative sampling procedure which usually ensures spectra of sufficient quality to permit unequivocal assignments.

There are no reports on the electronic spectra of the rhenium oxide fluorides, and only a single paper on the gas-phase UV/VIS spectrum of MnO_3F.[14] Vibrational data have been reported for *molecular* MnO_3F, ReO_3F, ReO_2F_3 and $ReOF_5$. In the present study matrix IR experiments have been used to establish the purity and the appropriate spray-on conditions most suitable for isolating monomeric species and subsequent to carrying out the UV/VIS investigation.

Experimental

Sample Preparation.—The compounds were prepared by modifications of literature methods.[5,15–17] Volatiles were manipulated using a stainless-steel manifold fitted with high-pressure valves (Autoclave Engineers). Solid materials were handled in a dry-box (< 5 ppm H_2O).

MnO_3F. **CAUTION**: when pure, quantities of greater than 1 g of MnO_3F can detonate with extreme violence.

This compound was prepared by the reaction of $KMnO_4$ (1.2 g, 7.6 mmol) with a slight excess of IF_5 (Fluorochem) at room temperature in prefluorinated stainless-steel or F.E.P. reactors. It was readily purified by vacuum sublimation onto $KMnO_4$ in a second F.E.P. reactor and leaving to stand for 3 h at room temperature. Pure, dark green MnO_3F was then transferred by vacuum sublimation at *ca.* 253 K into a prefluorinated nickel can fitted with a brass bellows valve (Hoke, M2172B) and stored for up to 7 d.

ReO_3F. This was prepared by the reaction of $KReO_4$ (1 g, 3.5 mmol) (Aldrich) with excess of IF_5 and a trace of HF at 373 K for 16 h in a glass reactor fitted with a poly(tetrafluoroethylene) (ptfe) tap (Young Scientific). Under perfectly anhydrous conditions, $KReO_4$ and IF_5 do not react, and a catalytic quantity of HF is essential. Pale yellow solid ReO_3F was isolated by sublimation under dynamic vacuum in glass after the excess of IF_5 had been pumped away.

ReO_2F_3. The compound Re_2O_7 (1.3 g, 2.7 mmol) was loaded into a stainless-steel autoclave (150 cm^3) with fluorine [450 cm^3, 3 atm (*ca.* 3 × 10^5 Pa)] and the mixture heated to 473 K for 16 h. After removal of the volatiles *in vacuo*, the autoclave was opened in the dry-box and pale yellow ReO_2F_3 scraped from the inner surface and stored in prefluorinated F.E.P. containers.

$ReOF_5$. This was prepared by the static fluorination of ReO_2 (0.7 g, 3.2 mmol) at 523 K in a prefluorinated nickel reactor. Volatile fractions were flashed off at room temperature until all the ReF_6 contaminant was removed. The $ReOF_5$ was then transferred by vacuum sublimation to a prefluorinated nickel can for storage.

$ReOF_4$. Rhenium powder (0.11 g, 0.6 mmol) (Aldrich) was activated by static hydrogenation at 573 K and then loaded into a stainless-steel autoclave (150 cm^3) with $ReOF_5$ (1 g, 3.4 mmol) and the mixture heated to 473 K for 16 h. At the end of this period the autoclave was cooled to room temperature and the volatiles (ReF_6 and unreacted $ReOF_5$) were removed *in vacuo*. The autoclave was opened in a dry-box and blue $ReOF_4$ scraped from the inner surface and stored in prefluorinated F.E.P. containers.

Techniques.—The general features of our matrix-isolation IR and UV/VIS equipment have been described elsewhere.[6] Nitrogen and argon (BOC 99.999%) were used as matrix gases, and samples were deposited onto an optically transparent window cooled to *ca.* 12 K. Infrared studies were carried out using a Perkin-Elmer PE 983G spectrometer and CsI optics. The UV/VIS studies employed LiF optics and a PE 554 spectrometer.

The compounds $ReOF_5$ and MnO_3F were introduced into the matrix apparatus by vaporisation directly from their nickel storage cans at *ca.* 251 and 178 K respectively *via* a brass inlet system. In separate experiments, to avoid handling large quantities of the material, MnO_3F was prepared *in situ* on the matrix-isolation vacuum shroud by the reaction of $KMnO_4$ with HSO_3F at 273 K. The volatile MnO_3F was vaporised directly onto the cold window. Initial attempts to record good-quality spectra from ReO_3F, ReO_2F_3 and $ReOF_4$ were unsuccessful due to decomposition, during spray-on, at surfaces which could not be adequately passivated before cool down. The glass apparatus shown in Fig. 1 was designed to avoid this complication. It was pumped to high vacuum and passivated sequentially with fluorine (twice) and ClF_3. Samples of ReO_3F,

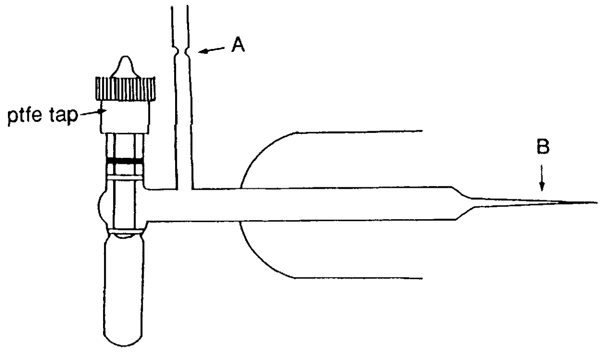

Fig. 1 Spray-on apparatus for moisture-sensitive solid samples

Table 1 Prominent IR bands (cm^{-1}) observed in matrix-isolation studies on manganese and rhenium oxide fluorides

Compound	This work[a]	Previous work	Assignment
MnO_3F (C_{3v})	953	951[b]	$\nu_4(E)$
	904	904[b]	$\nu_1(A_1)$
	717	716[b]	$\nu_2(A_1)$
	380	380[b]	$\nu_5(E)$
	340	339[b]	$\nu_3(A_1)$
	—	264[b]	$\nu_6(E)$
ReO_3F (C_{3v})	1018	1017[c]	$\nu_1(A_1)$
	982	983[c]	$\nu_4(E)$
	702	701[c]	$\nu_2(A_1)$
	—	354[c]	$\nu_5(E)$
	319	318[c]	$\nu_3(A_1)$
	229	237[c]	$\nu_6(E)$
ReO_2F_3 (C_{2v})	1029	1029[c]	$\nu_1(A_1)$
	992	992[c]	$\nu_{10}(B_2)$
	701	701[c]	$\nu_2(A_1)$
	674	674[c]	$\nu_7(B_1)$
	621	621[c]	$\nu_4(A_1)$
	—	286[c]	$\nu_8(B_1)$
	—	271[c]	$\nu_{11}(B_2)$
	—	260[c]	$\nu_{12}(B_2)$
	—	252[c]	$\nu_9(B_1)$
$ReOF_5$ (C_{4v})	997	991[d]	$\nu_1(A_1)$
	737	738[d]	$\nu_2(A_1)$
	708	713[d]	$\nu_8(E)$
	620	643[d]	$\nu_3(A_1)$
	—	365[d]	$\nu_{10}(E)$
	306	309[d]	$\nu_4(A_1)$
	257	260[d]	$\nu_9(E)$
$ReOF_4$ (C_{4v})	1082	1080[e] 1072[f]	$\nu_1(A_1)$
	710	722[e] 701[f]	$\nu_7(E)$
	685	696[e] 667[f]	$\nu_2(A_1)$
	—	484[e] —	—
	302	— 303[f]	$\nu_8(E)$
	245	— 245[f]	$\nu_9(E)$

[a] Nitrogen matrix, frequency accuracy ± 1 cm^{-1}. [b] Data taken from ref. 2. [c] Data taken from ref. 3. [d] Data taken from ref. 5. [e] Matrix data taken from ref. 4. [f] HF solution data taken from ref. 4.

ReO_2F_3 and $ReOF_4$ were then loaded into it in the dry-box *via* a prefluorinated glass funnel inserted through the barrel of the ptfe tap. The apparatus was then pumped to high vacuum and sealed at A. The whole apparatus was transferred to the matrix-isolation vacuum shroud and, after cool down, the Displex head was rotated breaking the break-seal B and affording a completely passivated surface directly onto the cold window. In this way, highly reactive fluorides may be studied with minimal decomposition problems. In this work, ReO_3F, ReO_2F_3 and $ReOF_4$ were sublimed at *ca.* 323, 313 and 273 K respectively.

Results and Discussion

Infrared Spectroscopic Studies.—MnO_3F. Previous microwave[18] and both gas-phase[1] and matrix-isolation infrared studies[2] on MnO_3F have established that this molecule exists as a monomer possessing C_{3v} symmetry in the vapour phase. When either prepared samples of MnO_3F or the vapour species above mixtures of potassium permanganate and fluorosulphonic acid, held at *ca.* 270 K, were isolated in nitrogen matrices, absorptions were observed at 953, 904 and 717 cm^{-1} with additional weaker features at 380 and 340 cm^{-1}. All five of these absorptions correspond well with those previously assigned to monomeric MnO_3F, Table 1, and demonstrate that both of these routes give rise to monomeric MnO_3F essentially free of any impurity.

ReO_3F. The infrared spectrum of matrix-isolated samples of ReO_3F has been reported previously.[3] Such spectra exhibit six bands which are assigned to the infrared fundamentals of ReO_3F adopting C_{3v} symmetry. Table 1 compares our data for matrix-isolated ReO_3F with that reported previously[3] where five of the six infrared fundamentals of C_{3v} ReO_3F are observed, indicating that our spectra are essentially free of any impurity.

ReO_2F_3. The previous matrix-isolation study on this compound utilising oxygen-18 enrichment and force-field analyses by this group concluded that monomeric ReO_2F_3 adopts a trigonal bipyramidal-based structure with overall C_{2v} symmetry.[3] The observed infrared stretching frequencies were assigned on this basis as follows: 1029 [A_1, ν(Re=O)], 992 [B_2, ν(Re=O)], 701 [A_1, $\nu(Re-F_{eq})$], 674 [B_1, ν(Re–F)] and 621 cm^{-1} [A_1, ν(Re–F)]. Survey spectra recorded after initial deposition of our samples also exhibited bands due to these stretching modes but, in addition, a further peak in the rhenium–oxygen stretching region at *ca.* 983 cm^{-1} was observed. As deposition continued, growth of the bands assigned to ReO_2F_3 overtook that of this impurity band until eventually they dominated the spectrum. Such behaviour is typical of a decomposition product, and we can identify the band at 983 cm^{-1} as the E mode of ReO_3F, which arises, presumably, from partial hydrolysis of ReO_2F_3 on parts of the matrix vacuum shroud which could not be prefluorinated. As a result of this hydrolysis it proved impossible to obtain an infrared spectrum which was *totally* free of ReO_3F impurity in the initial stages of deposition.

$ReOF_5$. This compound has not previously been studied by matrix-isolation infrared spectroscopy although its gas-phase IR and solid-state Raman spectrum have been reported and interpreted on the basis of a C_{4v} monomer.[5] In that study all the fundamental frequencies were identified and assigned. In particular, infrared-active stretching modes were observed at 991 [A_1, ν(Re=O)], 738 [A_1, ν(Re–F)], 713 [E, ν(Re–F)] and 643 cm^{-1} [A_1, ν(Re–F)]. Fig. 2(*a*) shows a typical spectrum obtained after codeposition of $ReOF_5$ and nitrogen. We observe corresponding stretching modes at 996.9, 736.9, 707.6 and 620.0 cm^{-1}, demonstrating that $ReOF_5$ has been isolated as a monomer under our conditions.

$ReOF_4$. The vibrational spectrum of this material has been studied both as a solid and in HF solution. Additionally a low-resolution matrix-isolation experiment in argon has been reported.[4] This latter study identified rhenium–oxygen and rhenium–fluorine infrared-active stretching modes at 1080 [A_1, ν(Re=O)], 722 [E, ν(Re–F)] and 696 cm^{-1} [A_1, ν(Re–F)] which when coupled with their Raman experiments allowed assignment on the basis of C_{4v} monomeric $ReOF_4$, as subsequently confirmed for other transition-metal oxide tetrafluorides.[6,11,19] Spectra obtained from our matrix studies showed corresponding absorptions at 1082.0, 710.4 and 685.4 cm^{-1}, Fig. 2(*b*). In addition we observed two further bands at 301.5 and 245.0 cm^{-1} which may be assigned to bending modes by comparison with Raman spectra recorded on the solid. The previous matrix-isolation study by Paine *et al.* was limited to the spectra region 4000–400 cm^{-1} and hence did not yield frequencies for the bending modes. However, a weak band at *ca.* 484 cm^{-1} was observed in that study which could not be assigned by comparison with the data from solid and HF solution work. We have not been able to reproduce this band in any of our studies and suggest that it arose from some impurity.

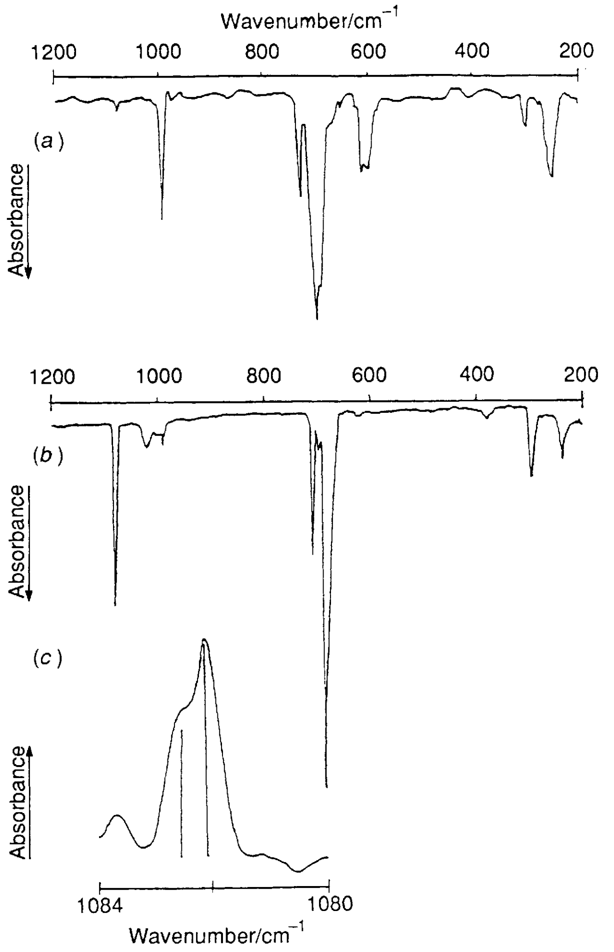

Fig. 2 (*a*) Low-resolution spectrum recorded after co-condensing $ReOF_5$ and nitrogen at *ca.* 12 K. (*b*) Low-resolution spectrum of $ReOF_4$ matrix-isolated in nitrogen. (*c*) High-resolution spectrum (1084–1080 cm^{-1}) of the rhenium–oxygen stretching mode for $ReOF_4$ isolated in a nitrogen matrix

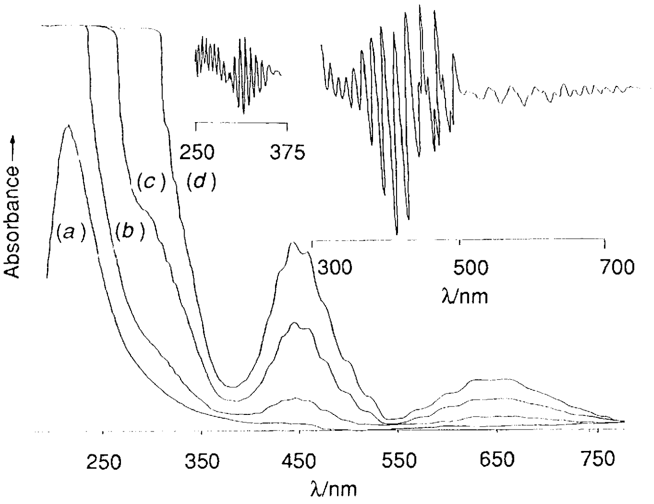

Fig. 3 The UV/VIS spectra of MnO_3F isolated in a nitrogen matrix: (*a*) 5 s spray; (*b*) 15 s spray; (*c*) 60 s spray; (*d*) 3 min spray. Inset: 250–730 nm with derivative recording

Fig. 2(*c*) shows the effect of recording the band centred at *ca.* 1082 cm^{-1} under higher resolution. This band now appears as two partially resolved peaks centred at 1082.5 and 1082.1 cm^{-1} in the approximate intensity ratio of 2:3. This splitting fits, both in terms of intensity and magnitude, that calculated for a diatomic ReO unit (natural abundance of rhenium-185, 37.4; -187, 62.6%; calculated splitting 1082.5 and 1082.0 cm^{-1}). The relatively good agreement between the observed values and those obtained from simple reduced-mass calculations suggests that the interaction between the A_1 rhenium–oxygen and rhenium–fluorine modes is relatively small. Unfortunately, we were unable to resolve similar isotopic splittings on any of the other bands which could then be used to obtain a value for the O–Re–F bond angle. However, it is possible to make an estimate of the angle between the C_4 axis and the rhenium–fluorine bond, θ, from the observed relative intensities of the A_1 and E rhenium–fluorine stretching modes, provided the interaction between the two A_1 stretching modes is assumed to be zero. It has been shown, for the analogous $CrOF_4$ molecule,[10] that, under these conditions, the intensity ratio is given by equation (1).

$$\frac{I_E}{I_{A_1}} = \tan^2\theta\left(\frac{1}{M_F}+\frac{2\sin^2\theta}{M_{Re}}\right)\Bigg/\left(\frac{1}{M_F}+\frac{4\cos^2\theta}{M_{Re}}\right) \qquad (1)$$

The ratio of the areas under the E and A_1 bands in the spectra was measured as 9.7:1, from which a value of 71° is calculated for θ and thus the O–Re–F angle may be estimated as 109°. There are a number of sources of errors in such calculations. The inherent approximations in deriving the formulae for the intensities of the bands, such as neglect of anharmonicity, the factoring of stretching and bending modes and the lack of interaction between the two A_1 symmetry stretching modes. There is also an attendant error in estimating the area under the two peaks. Considering these factors, it is prudent to place an error limit of at least ±6° on the derived value. However, the angle obtained appears reasonable when compared with the values obtained by electron diffraction for $CrOF_4$ (104°), $MoOF_4$ (104°) and WOF_4 (104°)[19] and from vibrational data for $RuOF_4$ (100°).[20]

UV/VIS Spectra.—The electronic spectra of monomeric MnO_3F, ReO_3F, ReO_2F_3, $ReOF_5$ and $ReOF_4$ isolated in nitrogen matrices at 12 K were recorded over the range 190–850 nm (*ca.* 52 000–12 000 cm^{-1}). Typical spectra are shown in Figs. 3–7, and the band positions are in Table 2.

The UV/VIS spectra for metal oxide halides may in principle be interpreted by molecular orbital (MO) calculations[21] (*e.g.* SCF-X_α-SW calculations) and the optical electronegativity model for the prediction of the lowest-energy charge-transfer transitions. No MO calculations for the rhenium oxide fluorides have been carried out, so we have used the latter approach.

MnO_3F. The UV/VIS spectrum (Fig. 3) of matrix-isolated monomeric MnO_3F (C_{3v}) is comparable to the reported gas-phase spectrum.[14] The spectrum of the matrix-isolated monomer shows five features at 15 500, 22 300, 33 300, 40 000 (sh) and 46 200 cm^{-1}, the four lower-energy bands showing very well resolved fine structure. The provision of second-derivative recording (inset) allows this vibrational fine structure to be resolved giving progressions of 830, 780, 660 and 710 ± 20 cm^{-1} respectively, which may be correlated with the A_1 Mn=O stretch at 904 cm^{-1} and the A_1 Mn–F stretch at 717 cm^{-1}. These allow the bands at 15 500, 22 300 and 40 000 cm^{-1} to be unequivocally assigned as O→Mn charge-transfer transitions, and that at 33 300 cm^{-1} as a F→Mn charge-transfer transition.

ReO_3F. The UV/VIS spectrum (Fig. 4) of matrix-isolated monomeric ReO_3F may be assigned by direct comparison with the tetrahedral perrhenate anion.[22] The similarity of the spectra for these compounds (both show two intense bands at *ca.* 43 000 and 47 000 cm^{-1}) allows both bands to be identified as O→Re charge-transfer transitions. For ReO_3F a vibrational progression of 880 ± 20 cm^{-1} on the lower-energy band, which may be correlated with the A_1 Re=O stretch at 1018 cm^{-1}, confirms this assignment.

ReO_2F_3. As indicated earlier, ReO_3F was present as a persistent impurity in all matrix experiments on ReO_2F_3. In the UV/VIS region this compound exhibits two intense absorp-

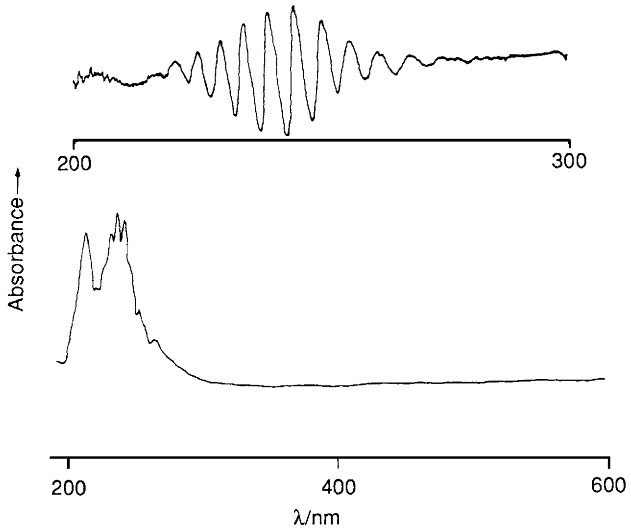

Fig. 4 The UV/VIS spectrum (lower) of ReO_3F isolated in a nitrogen matrix; upper trace shows derivative recording over the range 200–300 nm

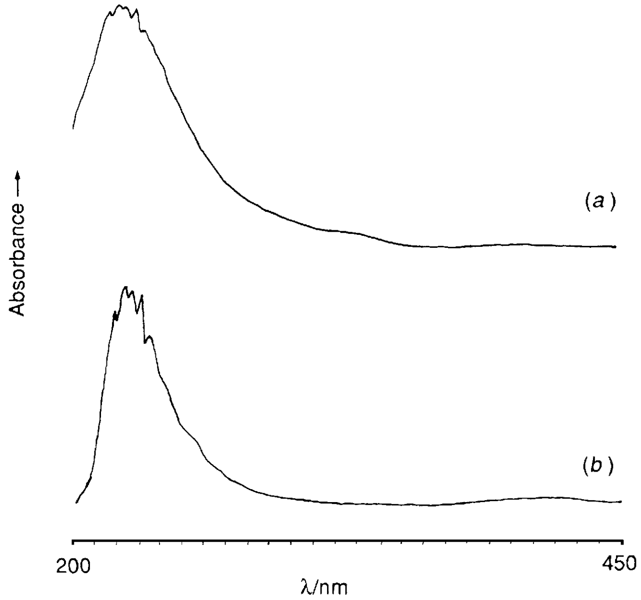

Fig. 5 (*a*) A typical UV/VIS spectrum obtained from vaporisation of ReO_2F_3 in a nitrogen matrix. (*b*) Spectrum of ReO_2F_3 monomer obtained after subtraction of ReO_3F (Fig. 4)

tions, and spectral subtraction (with different weightings) was necessary to remove these absorptions. We have already shown the usefulness and reproducibility of this technique by the removal of small, but varying, amounts of OsO_4 from the UV/VIS spectra of the osmium oxide fluorides,[12] and are confident that the procedure does not produce artefacts.

A typical experimental UV/VIS spectrum of ReO_2F_3 and the spectrum after spectral subtraction of ReO_3F are shown in Fig. 5. Three bands are observed but, unfortunately, only the most intense feature (44 200 cm^{-1}) shows any resolvable fine structure. The latter corresponds to a progression of 880 ± 20 cm^{-1} which correlates with the A_1 (Re=O) stretch at 1029 cm^{-1} and identifies this unequivocally as an O⟶Re charge-transfer transition.

$ReOF_5$. The UV/VIS spectrum of $ReOF_5$ (Fig. 6) is qualitatively very similar to that of ReO_2F_3, showing bands at 37 500, 41 500 and 46 200 cm^{-1} with an additional intense feature at 51 700 cm^{-1}.

$ReOF_4$. Rhenium(VI) has the [Xe]$5d^1$ configuration and in C_{4v} symmetry the d-orbital ordering expected is $d_{xy}(b_2) < d_{xz},d_{yz}(e) < d_{x^2-y^2}(b_1) < d_{z^2}(a_1)$ with the ground state $d_{xy}^{\,1}$.

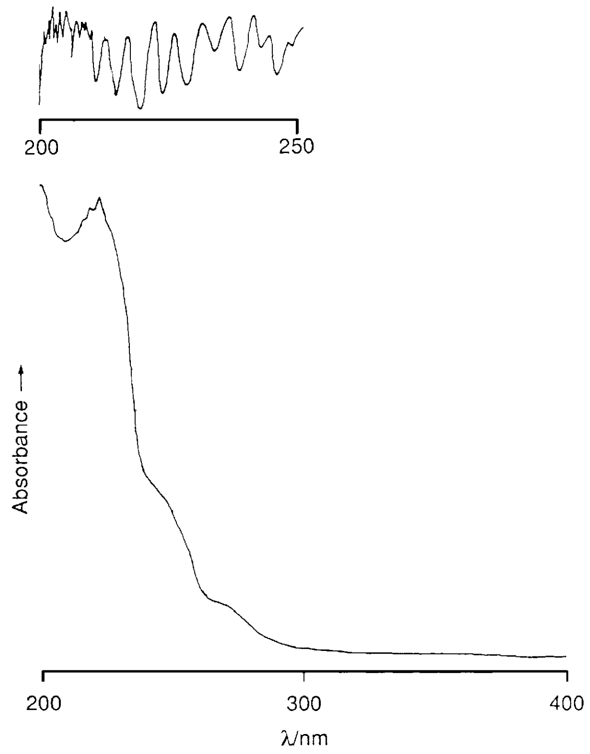

Fig. 6 The UV/VIS spectrum (lower) of $ReOF_5$ isolated in a nitrogen matrix; upper trace shows derivative recording over the range 200–250 nm

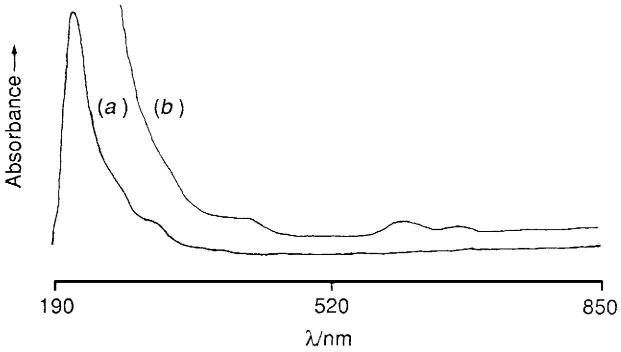

Fig. 7 The UV/VIS spectra of $ReOF_4$ (*a*) isolated in a nitrogen matrix, (*b*) after prolonged deposition

The UV/VIS spectrum of $ReOF_4$ (Fig. 7) shows six bands, an intense feature at 46 100 cm^{-1} with a distinct shoulder at 37 400 cm^{-1}, and four weaker features at 32 400, 25 000, 16 300 and 14 600 cm^{-1}. Unfortunately, none of these shows any resolvable fine structure. We tentatively assign the four weaker features as d–d transitions. The $b_2 \longrightarrow e$ transition in the isostructural $OsOF_4$ has been observed at ≈16 000 cm^{-1},[12] while $10Dq$ for the isoelectronic ReF_6 is ≈28 000 cm^{-1} suggesting a range of 25 000–31 000 cm^{-1} for the $b_2 \longrightarrow a_1$ separation in $ReOF_4$. This allows us to make tentative assignments for the bands at 14 600 and 16 300 cm^{-1} as $b_2 \longrightarrow e$ (split), 25 000 cm^{-1} as $b_2 \longrightarrow b_1$ and 32 400 cm^{-1} as $b_2 \longrightarrow a_1$. The remaining features are charge-transfer transitions.

χ_{opt} *Considerations*.—The optical electronegativity model allows for the prediction of the lowest-energy charge-transfer transitions in metal complexes using equation (2). Despite

$$E/\mathrm{cm}^{-1} = 30\,000[\chi_{opt}(\mathrm{X}) - \chi_{opt}(\mathrm{M})] \qquad (2)$$

the inherent simplicity, this model works well for many systems including metal binary fluorides and metal oxide chlorides. However, it has given poor predictions for metal oxide fluorides,[23] *e.g.* taking $\chi_{opt}(F^-)$ as 3.9 and $\chi_{opt}(Mo^{VI})$ as 2.1[22] the optical electronegativity model predicts the lowest F $\longrightarrow$ Mo transition at 54 000 cm^{-1}, as compared with the observed transition at 39 150 cm^{-1}.[11] Furthermore, the establishment of a value for the optical electronegativity of the O^{2-} ion is difficult,[22] since as a result of $M_{d\pi}$–$O_{p\pi}$ interactions, $\chi_{opt}(O^{2-})$ varies both with the metal and with the number of oxide ligands. Values of *ca.* 3.2–3.5 have been suggested for different systems resulting in a spread of ≈9000 cm^{-1} in predicted O⟶M charge-transfer transitions. As a result of the present and past work[6,11,12] there are now sufficient data to test the model for metal oxide fluorides and, if necessary, to propose empirical modifications.

The optical electronegativities of five- and six-co-ordinate transition metals derived from their binary fluorides, and those of tetrahedral four-co-ordinate transition metals derived from their tetraoxo $[MO_4]^{n-}$ complexes are in Table 3. It should be noted that these values have been corrected, where appropriate, for spin-pairing effects, but not for spin–orbit effects. This is quite reasonable since although these effects are of comparable magnitude the very limited d–d data for the oxide fluorides precludes making spin–orbit corrections for these complexes. Taking these values of $\chi_{opt}(M^{n+})$ and the lowest experimentally observed charge-transfer bands allows the calculation of $\chi_{opt}(F^-)$ and $\chi_{opt}(O^{2-})$ for a range of transition metal oxide fluorides (Table 3).

Table 2 UV/VIS spectral data for manganese and rhenium oxide fluorides isolated in low-temperature matrices

Compound	E_{max}[a] (cm^{-1})	Vibrational spacing[b] (cm^{-1})	Assignment
MnO_3F	46 200 (216)	—	—
	40 000 (sh)	710	σ(O)⟶Mn c.t.
	33 300 (300)	660	π(F)⟶Mn c.t.
	22 300 (448)	780	π(O)⟶Mn c.t.
	15 500 (645)	830	π(O)⟶Mn c.t.
ReO_3F	47 000 (213)	—	π(O)⟶Re c.t.
	42 300 (236)	880	π(O)⟶Re c.t.
ReO_2F_3	44 200 (226)	880	π(O)⟶Re c.t.
	41 300 (242)	—	π(F)⟶Re c.t.
	38 000 (263)	—	π(O)⟶Re c.t.
$ReOF_5$	51 700 (193)	—	—
	46 200 (216)	940	π(O)⟶Re c.t.
	41 500 (sh)	—	π(F)⟶Re c.t.
	37 500 (sh)	—	π(O)⟶Re c.t.
$ReOF_4$	46 100 (217)	—	π(F)⟶Re c.t.
	37 400 (267)	—	π(O)⟶Re c.t.
	32 400 (309)	—	$b_2 \longrightarrow a_1$
	25 000 (400)	—	$b_2 \longrightarrow b_1$
	16 300 (613)	—	$b_2 \longrightarrow e$
	14 600 (685)	—	

c.t. = Charge transfer. [a] Nitrogen matrix, frequency accuracy ±100 cm^{-1}. Peak maxima in nm in parentheses. [b] Frequency accuracy ±20 cm^{-1}.

For d^0 transition-metal complexes the calculations are straightforward using equation (2). For $ReOF_4$ and $OsOF_5$, rhenium(VI) and osmium(VII) have the [Xe]5d^1 configuration, and in C_{4v} symmetry the d-orbital ordering expected is $d_{xy}(b_2) < d_{xz},d_{yz}(e) < d_{x^2-y^2}(b_1) < d_{z^2}(a_1)$ with the ground state $d_{xy}{}^1$. Therefore, in any calculations of χ_{opt} a correction for spin pairing must be applied. For $ReOF_4$ and $OsOF_5$ the spin-pairing energy is $\frac{4}{3}D$. Although D is unknown for these complexes, it should be comparable to ReF_6, for which $D \approx 2500$ cm^{-1}.[7] Hence equation (2) becomes (3).

$$E/\text{cm}^{-1} = 30\,000[\chi_{opt}(X) - \chi_{opt}(M)] + 3300 \qquad (3)$$

For d^2 (C_{4v}) $OsOF_4$, the ground-state configuration is $d_{xy}{}^2$ and the lowest possible charge-transfer transitions are to d_{xz},d_{yz}. Any calculations of χ_{opt} must therefore include contributions from both the d_{xy}–d_{xz},d_{yz} separation and spin pairing. A weak feature at 16 600 cm^{-1} has been assigned to the $d_{xy} \longrightarrow d_{xz},d_{yz}$ transition in $OsOF_4$,[12] while the spin-pairing energy for the d^2 $OsOF_4$ is $-\frac{1}{3}D$. Again, D for $OsOF_4$ is unknown, but should be comparable to the values for ReF_6, OsF_6, $ReOF_4$ and $OsOF_5$, and we have taken a value of $D \approx 2500$ cm^{-1}. Hence, equation (2) becomes (4).

$$E/\text{cm}^{-1} = 30\,000[\chi_{opt}(X) - \chi_{opt}(Os^{VI})] + 15\,800 \qquad (4)$$

The values of $\chi_{opt}(O^{2-})$ satisfactorily lie in the ranges expected[22] for four-co-ordinate complexes (3.0–3.2) and five- and six-co-ordinate complexes (3.4–3.5) confirming that the $\chi_{opt}(M^{n+})$ values are reasonable. The agreement for OsO_3F_2 however is poor. For this complex the effect of $M_{d\pi}$–$O_{p\pi}$ interactions for three oxygens must significantly decrease $\chi_{opt}(Os^{VIII})$ [NB bearing in mind the change in geometry, the co-ordination of four oxygens to Os^{VIII} in tetrahedral OsO_4 gives $\chi_{opt}(Os^{VIII}) = 2.1$[22]]. Taking the accepted value for $\chi_{opt}(O^{2-})$ of 3.5, we can make an estimate of these $M_{d\pi}$–$O_{p\pi}$ interactions, and calculate a better value for $\chi_{opt}(Os^{VIII})$ in OsO_3F_2 of 2.5 (Table 3).

The newly calculated values of $\chi_{opt}(F^-)$ (3.4–3.7) are remarkably constant across the range of complexes studied, bearing in mind the simplicity of the theory. Once again,

Table 3 Optical electronegativity calculations for transition-metal oxide fluorides

Compound	$\chi_{opt}(M^{n+})$	Lowest-energy F⟶M c.t. band (cm^{-1})	$\chi_{opt}(F^-)$ (calc.)	Lowest-energy O⟶M c.t. band (cm^{-1})	$\chi_{opt}(O^{2-})$ (calc.)	Ref.[a]
CrO_2F_2	2.2	29 500	3.4	21 000	2.9	24
$CrOF_4$	2.7	27 000	3.6	22 000	3.4	6
$MoOF_4$	2.1	39 150	3.4	Not observed	—	11
WOF_4	2.0	43 500[b]	3.5	Not observed	—	11
MnO_3F	2.55	33 300	3.7	15 500	3.1	*c*
ReO_3F	1.75	Not observed	—	42 300	3.2	*c*
ReO_2F_3	2.25[d]	41 500	3.6	38 000	3.5	*c*
$ReOF_5$	2.25[d]	41 500	3.6	37 500	3.5	*c*
$ReOF_4$	2.2	46 100	3.6	37 400	3.3	*c*
OsO_3F_2	2.7[e]	35 300	3.9	28 800	3.7	12
	2.5[f]	35 300	3.7	28 800	3.5	
$OsOF_5$	2.7[e]	31 750	3.6	27 500	3.5	12
$OsOF_4$	2.6	46 700	3.6	41 700	3.5	12

[a] References refer to papers where experimental data are reported. [b] There is a typographical error in Table 2, ref. 11. Fig. 2(*b*) in the same paper clearly shows the electronic transition for WOF_4 above 40 000 cm^{-1}. [c] This work. [d] Calculated from the electronic spectrum of ReF_7.[25] [e] χ_{opt} for Os^{VII} and Os^{VIII} estimated from osmium(VI) data.[12] [f] $\chi_{opt}(Os^{VIII})$ estimated from OsO_3F_2 taking $\chi_{opt}(O^{2-})$ as 3.5.

OsO_3F_2 is out of line with the other complexes, supporting the proposal that $\chi_{opt}(Os^{VIII})$ in OsO_3F_2 is less than 2.7. Using the new value of $\chi_{opt}(Os^{VIII})$ calculated from the oxygen data above gives a reasonable value for $\chi_{opt}(F^-)$ of 3.7. It would appear that, in high-oxidation-state transition-metal complexes, $M_{d\pi}$–$F_{p\pi}$ interactions are significant such that $\chi_{opt}(F^-)$ also varies with the metal and the nature of the coligands. We propose that a value of $\chi_{opt}(F^-)$ of 3.6–3.7 is more appropriate for transition-metal oxide fluorides, and that this modified value will be of some value not only in spectral interpretation, but also in predicting the positions of charge-transfer bands for other oxide fluorides.

Acknowledgements

We thank the SERC for financial support.

References

1 E. L. Varetti, R. R. Filgueira and A. Müller, *Spectrochim. Acta, Part A*, 1981, **37**, 369.

2 M. J. Reisfeld, L. B. Asprey and N. A. Matwiyoff, *Spectrochim. Acta, Part A*, 1971, **27**, 765.

3 I. R. Beattie, R. A. Crocombe and J. S. Ogden, *J. Chem. Soc., Dalton Trans.*, 1977, 1481.

4 R. T. Paine, K. L. Treuil and F. E. Stafford, *Spectrochim. Acta, Part A*, 1973, **29**, 1891.

5 J. H. Holloway, H. Selig and H. H. Claassen, *J. Chem. Phys.*, 1971, **54**, 4305.

6 E. G. Hope, P. J. Jones, W. Levason, J. S. Ogden, M. Tajik and J. W. Turff, *J. Chem. Soc., Dalton Trans.*, 1985, 1443.

7 J. H. Holloway, G. Stanger, E. G. Hope, W. Levason and J. S. Ogden, *J. Chem. Soc., Dalton Trans.*, 1988, 1341.

8 A. K. Brisdon, P. J. Jones, W. Levason, J. S. Ogden, J. H. Holloway, E. G. Hope and G. Stanger, *J. Chem. Soc., Dalton Trans.*, 1990, 715.

9 E. G. Hope, *J. Chem. Soc., Dalton Trans.*, 1990, 723.

10 E. G. Hope, P. J. Jones, W. Levason, J. S. Ogden, M. Tajik and J. W. Turff, *J. Chem. Soc., Dalton Trans.*, 1985, 529.

11 W. Levason, R. Narayanaswamy, J. S. Ogden, A. J. Rest and J. W. Turff, *J. Chem. Soc., Dalton Trans.*, 1981, 2501.

12 E. G. Hope, W. Levason and J. S. Ogden, *J. Chem. Soc., Dalton Trans.*, 1988, 61.

13 E. G. Hope, W. Levason and J. S. Ogden, *J. Chem. Soc., Dalton Trans.*, 1988, 997.

14 J. P. Jasinski, S. L. Holt, J. H. Wood and J. W. Moskowitz, *J. Chem. Phys.*, 1975, **63**, 1429.

15 G. A. Yagodin, A. A. Opalovskii, E. G. Rakov and A. S. Dudin, *Dokl. Akad. Nauk SSSR*, 1980, **252**, 1400.

16 W. A. Sunder and F. A. Stevie, *J. Fluorine Chem.*, 1975, **6**, 449.

17 E. E. Aynsley and M. L. Hair, *J. Chem. Soc.*, 1958, 3747.

18 A. Javan and A. Engelbrecht, *Phys. Rev.*, 1954, **96**, 649.

19 J. Huang, K. Hedberg, J. M. Shreeve and S. P. Mallela, *Inorg. Chem.*, 1988, **27**, 4633; K. Iijima, *Bull. Chem. Soc. Jpn.*, 1977, **50**, 373; K. Iijima and S. Shibata, *Bull. Chem. Soc. Jpn.*, 1974, **47**, 1393; 1975, **48**, 666.

20 E. G. Hope, unpublished work.

21 L. Helmholz, H. Brennan and M. Wolfsberg, *J. Chem. Phys.*, 1955, **23**, 853.

22 C. K. Jørgensen, *Prog. Inorg. Chem.*, 1970, **12**, 101; A. Müller, E. Diemann and C. K. Jørgensen, *Struct. Bonding (Berlin)*, 1973, **14**, 23.

23 H. So and M. T. Pope, *Inorg. Chem.*, 1972, **11**, 1441.

24 J. P. Jasinski, S. L. Holt, J. H. Wood and L. B. Asprey, *J. Chem. Phys.*, 1975, **63**, 757.

25 E. G. Hope, W. Levason and J. S. Ogden, unpublished work.

Received 27th March 1991; *Paper* 1/01497H